

# LHC constraints on the Lee–Wick Higgs sector



Christopher D. Carone\*, Raymundo Ramos, Marc Sher

High Energy Theory Group, Department of Physics, College of William and Mary, Williamsburg, VA 23187-8795, United States

## ARTICLE INFO

### Article history:

Received 6 March 2014

Accepted 14 March 2014

Available online 20 March 2014

Editor: B. Grinstein

## ABSTRACT

We determine constraints on the Lee–Wick Higgs sector obtained from the full LHC Higgs boson data set. We determine the current lower bound on the heavy neutral Lee–Wick scalar, as well as projected bounds at a 14 TeV LHC with 300 and 3000 inverse femtobarns of integrated luminosity. We point out that the first sign of new physics in this model may be the observation of a deviation from standard model expectations of the lighter neutral Higgs signal strengths corresponding to production via gluon–gluon fusion and decay to either tau or Z pairs. The signal strength of the latter is greater than the standard model expectation, unlike most extensions of the standard model.

© 2014 The Authors. Published by Elsevier B.V. This is an open access article under the CC BY license (<http://creativecommons.org/licenses/by/3.0/>). Funded by SCOAP<sup>3</sup>.

## 1. Introduction

Over the past three decades, the most popular approach to addressing the hierarchy problem of the standard model has been to introduce additional particles whose virtual effects lead to a cancellation of quadratic divergences. Supersymmetry has been the most studied scenario of this type; only a few years ago, there was much anticipation that colored superparticles would be revealed early in the first run of the Large Hadron Collider (LHC). Unfortunately, this expectation has not been realized. Since theories with partner particles have a decoupling limit, it is possible that the colored partners, which the LHC is most capable of detecting, may lie just beyond the reach of the initial  $\sim 8$  TeV run. It also follows that alternatives to supersymmetry, with their own distinct set of partner particles, remain in play as possible solutions to the hierarchy problem. Here we determine how effectively current LHC data on the Higgs boson can constrain one such possibility, and explore the reach attainable in the future.

We assume the framework of the Lee–Wick Standard Model (LWSM) [1]. In the LWSM, a higher-derivative term quadratic in the fields is introduced for each standard model particle. An additional pole in each propagator corresponds to a new physical state, the Lee–Wick partner. Quadratic divergences in the theory are eliminated due to the faster fall-off of the momentum–space propagators in the higher-derivative formulation of the theory. The presence of twice as many time derivatives in the theory implies

that twice as much initial-value data is needed to specify solutions to the classical equations of motion. Hence, one anticipates that the theory can be reformulated in terms of an equivalent one with twice as many fields, but kinetic terms with only two derivatives. This is precisely what happens in the auxiliary-field formulation of the LWSM [1], as we will illustrate in the next section. The additional field corresponds to the Lee–Wick partner particle, and the elimination of quadratic divergences emerges via cancellations between diagrams involving ordinary and Lee–Wick particles, respectively [1].

The LWSM is unusual in that the Lee–Wick partner fields have wrong-sign quadratic terms; this implies that the Lee–Wick states have negative norm. In the original papers of Lee and Wick [2], as well as Cutkosky et al. [3], it was argued that the unitarity of such a theory could be maintained provided that the Lee–Wick partners are unstable (i.e., are excluded from the set of possible asymptotic scattering states) and that a specific pole prescription is used in evaluating loop diagrams. This approach has proven effective at the level it has been checked (one loop) and it is generally taken as a working assumption that some viable prescription exists at higher order. While Lee–Wick theories violate causality at a microscopic level, it has been argued that this may not lead to logical paradoxes [4]. In the context of scattering experiments, this has been supported by a study of the large- $N$  limit of the Lee–Wick  $O(N)$  model, where the unitarity and Lorentz-invariance of the S-matrix could be explicitly confirmed [5]. While the phenomenological implications of microscopic acausality are of substantial interest [6], they will not be the subject of this paper. Other phenomenological studies of Lee–Wick theories can be found in Ref. [7].

We focus instead on how the most current LHC data constrains the possibility of Lee–Wick partners. Specifically, we focus on a

\* Corresponding author.

E-mail addresses: [cddcaro@wm.edu](mailto:cddcaro@wm.edu) (C.D. Carone), [raramos@email.wm.edu](mailto:raramos@email.wm.edu) (R. Ramos), [mtsher@wm.edu](mailto:mtsher@wm.edu) (M. Sher).

Lee–Wick extension of the Higgs sector, an effective theory in which the Lee–Wick partner to the Higgs doublet is retained, while all the other Lee–Wick partners are assumed to be heavy and decoupled [8,9]. This approximation is justified for the following reason: the Lee–Wick partners to the Higgs field, the electroweak gauge bosons and the top quark are the most important in the cancellation of quadratic divergences; these would be expected to be the lightest to minimize fine tuning. Of this set, however, all but the partner to the Higgs doublet are forced up to multi-TeV energy scales by existing electroweak constraints [11]. As we will show in the next section, the Lee–Wick Higgs sector presents itself as an unusual, constrained two-Higgs doublet model, one that is specified by a single free parameter once the lightest scalar mass eigenvalue is fixed. Current data on the 125 GeV Higgs boson at the LHC can then be used to determine bounds on the masses of the other neutral and charged scalar mass eigenstates in the theory. We note that past studies of the Lee–Wick Higgs sector [8–10] were undertaken before LHC Higgs boson data was available; in this Letter we take into account all such data available to date and determine projected bounds based on current assessments of the integrated luminosities that may be realistically obtained.

Our Letter is organized as follows: In Section 2, we define our effective theory. In Section 3, we determine bounds on the heavier neutral scalar by fitting the model's predictions for the 125 GeV mass eigenstate, using the full data set currently available from the LHC. In the second part of this section, we determine projected bounds based on the assumption of 300 to 3000 fb<sup>-1</sup> of integrated luminosity at a 14 TeV LHC. In Section 4, we summarize our results and compare them to other existing bounds on the model.

## 2. The Lee–Wick Higgs sector

In the Higgs sector of our model, a higher-derivative kinetic term is included in the Higgs field Lagrangian

$$\mathcal{L} = (D_\mu \hat{H})^\dagger (D^\mu \hat{H}) - \frac{1}{m_h^2} (D_\mu D^\mu \hat{H})^\dagger (D_\nu D^\nu \hat{H}) - V(\hat{H}). \quad (2.1)$$

Here  $D_\mu = \partial_\mu - igW_\mu^a T^a - ig'B_\mu Y$  is the usual covariant derivative for the standard model gauge group and a hat denotes a field in the higher-derivative formulation of the theory. The Higgs potential is given by

$$V(\hat{H}) = \frac{\lambda}{4} \left( \hat{H}^\dagger \hat{H} - \frac{v^2}{2} \right)^2. \quad (2.2)$$

Eq. (2.1) is reproduced from the following Lagrangian,

$$\mathcal{L} = (D_\mu \hat{H})^\dagger (D^\mu \hat{H}) + [(D_\mu \tilde{H})^\dagger (D^\mu \tilde{H}) + \text{h.c.}] + m_h^2 \tilde{H}^\dagger \tilde{H} - V(\hat{H}), \quad (2.3)$$

if one eliminates the auxiliary field  $\tilde{H}$  using its equation of motion. If instead, one uses the field redefinition  $\hat{H} = H - \tilde{H}$ , Eq. (2.3) takes the standard Lee–Wick form

$$\mathcal{L}_{\text{LW}} = (D_\mu H)^\dagger (D^\mu H) - (D_\mu \tilde{H})^\dagger (D^\mu \tilde{H}) + m_h^2 \tilde{H}^\dagger \tilde{H} - V(H - \tilde{H}). \quad (2.4)$$

In unitary gauge, the Higgs doublet can be decomposed

$$H = \begin{pmatrix} 0 \\ \frac{v+h}{\sqrt{2}} \end{pmatrix}, \quad \tilde{H} = \begin{pmatrix} \tilde{h}^+ \\ \frac{\tilde{h} + i\tilde{p}}{\sqrt{2}} \end{pmatrix}, \quad (2.5)$$

where  $v \approx 246$  GeV is the electroweak scale. Expanding the potential in terms of its quadratic, cubic and quartic parts, we find:

$$V^{(2)} = \frac{\lambda v^2}{4} (h - \tilde{h})^2 - \frac{m_h^2}{2} (\tilde{h}^2 + \tilde{p}^2 + 2\tilde{h}^+ \tilde{h}^-), \quad (2.6)$$

$$V^{(3)} = \frac{\lambda v}{4} (h - \tilde{h}) [(h - \tilde{h})^2 + \tilde{p}^2 + 2\tilde{h}^- \tilde{h}^+], \quad (2.7)$$

$$V^{(4)} = \frac{\lambda}{16} [(h - \tilde{h})^2 + \tilde{p}^2 + 2\tilde{h}^- \tilde{h}^+]^2. \quad (2.8)$$

Note that the Lee–Wick charged scalar and pseudoscalar Higgs fields have mass  $m_{\tilde{h}}$ , while there is mixing between the neutral scalar states  $h$  and  $\tilde{h}$ . Indicating the neutral mass eigenstates with the subscript 0, we define the mixing angle

$$\begin{pmatrix} h \\ \tilde{h} \end{pmatrix} = \begin{pmatrix} \cosh \alpha & \sinh \alpha \\ \sinh \alpha & \cosh \alpha \end{pmatrix} \begin{pmatrix} h_0 \\ \tilde{h}_0 \end{pmatrix}. \quad (2.9)$$

The symplectic rotation is necessary to preserve the relative sign between the ordinary and Lee–Wick kinetic terms. It follows from Eq. (2.6) that

$$\tanh 2\alpha = -\frac{2m_h^2/m_{\tilde{h}}^2}{1 - 2m_h^2/m_{\tilde{h}}^2} \quad \text{or} \quad \tanh \alpha = -m_{h_0}^2/m_{\tilde{h}_0}^2, \quad (2.10)$$

where  $m_h^2 \equiv \lambda v^2/2$  is the mass of the lighter Higgs scalar in the absence of mixing. The mass squared eigenvalues are defined by  $m_{h_0}^2$  and  $-m_{\tilde{h}_0}^2$ , so that the squared mass parameters appearing in Eq. (2.10) are all positive. Note that  $\alpha$  is always negative.

The same steps that led to Eq. (2.4) determine the form of the Yukawa couplings

$$\mathcal{L} = \frac{\sqrt{2}}{v} \bar{u}_R m_u^{\text{diag}} (H - \tilde{H}) i\sigma^2 Q_L - \frac{\sqrt{2}}{v} \bar{d}_R m_d^{\text{diag}} (H - \tilde{H})^\dagger V_{\text{CKM}}^\dagger Q_L - \frac{\sqrt{2}}{v} \bar{e}_R m_e^{\text{diag}} (H - \tilde{H})^\dagger \ell_L + \text{h.c.}, \quad (2.11)$$

where we have suppressed generation indices. Here  $Q_L \equiv (u_L, V_{\text{CKM}} d_L)$ ,  $\ell_L \equiv (e_L, \nu_L)$ , and all the fermion fields shown are in the mass eigenstate basis. The couplings of the neutral scalar mass eigenstates to fermions can now easily be extracted using Eqs. (2.5) and (2.9).

We define the quantity  $g_{XY}$  to be the ratio of a neutral scalar coupling in the Lee–Wick theory that we have defined to the same coupling of the Higgs boson in the standard model. Here  $X$  designates the scalar state (either  $h_0$  or  $\tilde{h}_0$ ) and  $Y$  specifies the coupling of interest (for example,  $t\bar{t}$ ,  $b\bar{b}$ ,  $\tau^+\tau^-$ ,  $W^+W^-$  or  $ZZ$ ). The neutral Higgs couplings to gauge boson pairs can be extracted from Eq. (2.4) and the couplings to fermions from Eq. (2.11). For example, we find

$$g_{h_0 t\bar{t}} = g_{h_0 b\bar{b}} = g_{h_0 \tau\tau} = e^{-\alpha}, \quad (2.12)$$

$$g_{h_0 WW} = g_{h_0 ZZ} = \cosh \alpha, \quad (2.13)$$

$$g_{\tilde{h}_0 t\bar{t}} = g_{\tilde{h}_0 b\bar{b}} = g_{\tilde{h}_0 \tau\tau} = -e^{-\alpha}, \quad (2.14)$$

$$g_{\tilde{h}_0 WW} = g_{\tilde{h}_0 ZZ} = \sinh \alpha. \quad (2.15)$$

Note that the couplings  $g_{h_0 WW}$  and  $g_{h_0 ZZ}$  are bigger than one, unlike most extensions of the standard model. These results provide most of what we need to modify known theoretical results for Higgs boson properties in the standard model to obtain those appropriate to the scalar states in the present theory. The one coupling that is more complicated to modify is the effective Higgs coupling to two photons; the relevant one-loop amplitude depends

on a sum of terms that are modified by different  $\alpha$ -dependent factors. To proceed, we write the relevant Lee–Wick Lagrangian terms as

$$\begin{aligned} \mathcal{L} = & -\frac{gm_f}{2m_W} e^{-\alpha} (h_0 - \tilde{h}_0) \bar{f} f \\ & + (\cosh \alpha h_0 + \sinh \alpha \tilde{h}_0) gm_W W^+ W^- \\ & - \left( \frac{1}{2} \frac{m_h^2}{m_{\tilde{h}}^2} e^{-\alpha} \right) \frac{gm_{\tilde{h}}^2}{m_W} (h_0 - \tilde{h}_0) \tilde{h}^- \tilde{h}^+. \end{aligned} \quad (2.16)$$

Presented in this form, coefficients can be easily matched to those of the effective Lagrangian assumed in Ref. [13] to compute contributions to  $h_0 \rightarrow \gamma\gamma$  from intermediate loop particles of various spins. After identifying the appropriate coupling factors, the only other modification that needs to be made to these generic formulae is that an additional minus sign must be included in the amplitude term corresponding to the charged Higgs loop; this takes into account the overall sign difference between ordinary and Lee–Wick propagators.

### 3. Bounds

The quantities that we compute for purpose of comparison to the experimental data are the signal strengths  $R_i^{\text{LW}}$ , each a specified Higgs boson production cross section times branching fraction normalized to the standard model expectation for the same quantity. We consider production via gluon–gluon fusion (ggF), vector-boson fusion (VBF), associated production with a  $W$  or  $Z$  boson (Vh) and production via the top quark coupling (tth), as well as combinations of these possibilities. In most cases, the ratio of Lee–Wick to standard model Higgs production cross sections reduces to a simple factor (for example,  $e^{-2\alpha}$  for ggF). In the case of inclusive production at the LHC, we find that the ratio is well approximated by

$$\frac{\sigma^{\text{LW}}}{\sigma^{\text{SM}}} = 0.88e^{-2\alpha} + 0.12 \cosh^2 \alpha, \quad (3.1)$$

for a center-of-mass energy of either 8 or 14 TeV. The coefficients in this expression were determined using numerical predictions for the different contributions to the standard model Higgs production cross section, given in Ref. [12].

A total of 33 signal strengths measured at ATLAS, CMS and the Tevatron were collected for analysis; they correspond to different channels of Higgs production and decay, and include the final states  $\gamma\gamma$ ,  $ZZ$ ,  $WW$ ,  $bb$  and  $\tau\tau$  (Table 1). The analysis performed here is analogous to others found in the literature [14–16]. These references considered conventional two-Higgs doublet models, with results plotted as a function of  $\alpha$  and  $\tan\beta$ . We have seen, however, that the Lee–Wick Higgs sector is determined by a single parameter  $\alpha$ ; as indicated by Eq. (2.10), this mixing angle is in one-to-one correspondence with the value of the heavy scalar mass  $m_{\tilde{h}_0}$  after one fixes  $m_{h_0}$  at its experimental value. Hence, we will present our results as 95% C.L. lower bounds on the heavy Lee–Wick scalar mass.

This analysis is presented in two parts: We first determine bounds using the most recent data for the Higgs boson signal strengths shown in Table 1. We then determine projected bounds at a 14 TeV LHC by assuming that the experimental data will converge on standard model central values and that the errors will scale in a simple way with the integrated luminosity.

To find a lower bound on  $m_{\tilde{h}_0}$  from the current signal strengths, we construct the  $\chi^2$  function

**Table 1**  
Measured Higgs signal strengths.

Decay	Production	Measured signal strength $R^{\text{meas}}$	
$\gamma\gamma$	ggF + tth	$1.6_{-0.3}^{+0.3+0.3}$ [ATLAS] [18]	
	VBF	$1.9_{-0.6}^{+0.8}$ [ATLAS] [19]	
	Vh	$1.3_{-1.1}^{+1.2}$ [ATLAS] [19]	
	Inclusive	$1.55_{-0.28}^{+0.33}$ [ATLAS] [19]	
	ggF + tth	$0.52 \pm 0.5$ [CMS] [20]	
	VBF + Vh	$1.48_{-1.07}^{+1.24}$ [CMS] [20]	
	Inclusive	$0.78_{-0.26}^{+0.28}$ [CMS] [20]	
	ggF	$6.1_{-3.2}^{+3.3}$ [Tevatron] [21]	
	$WW$	ggF	$0.82_{-0.32}^{+0.33}$ [ATLAS] [19]
		VBF	$1.4_{-0.6}^{+0.7}$ [ATLAS] [19]
VBF + Vh		$1.66 \pm 0.79$ [ATLAS] [22]	
Inclusive		$0.99_{-0.28}^{+0.31}$ [ATLAS] [19]	
ggF		$0.76 \pm 0.21$ [CMS] [23]	
ggF + VBF + Vh		$0.72_{-0.18}^{+0.20}$ [CMS] [24]	
ggF		$0.8_{-0.8}^{+0.9}$ [Tevatron] [21]	
$ZZ$	ggF + tth	$1.45_{-0.36}^{+0.43}$ [ATLAS] [19]	
	VBF + Vh	$1.2_{-0.9}^{+1.6}$ [ATLAS] [19]	
	Inclusive	$1.43_{-0.35}^{+0.40}$ [ATLAS] [19]	
	ggF	$0.9_{-0.4}^{+0.5}$ [CMS] [25]	
	VBF + Vh	$1.0_{-2.3}^{+2.4}$ [CMS] [25]	
$bb$	Inclusive	$0.93_{-0.23}^{+0.26+0.13}$ [CMS] [26]	
	Vh	$0.2 \pm 0.5 \pm 0.4$ [ATLAS] [27]	
$\tau\tau$	Vh	$1.0 \pm 0.5$ [CMS] [28]	
	Vh	$1.56_{-0.73}^{+0.72}$ [Tevatron] [21]	
	Vh	$1.1_{-1.0}^{+1.3}$ [ATLAS] [29]	
$\tau^+\tau^-$	VBF	$-0.4 \pm 1.5$ [ATLAS] [30]	
	VBF + Vh	$1.6_{-0.7}^{+0.8}$ [ATLAS] [29]	
	ggF + VBF + Vh	$1.4_{-0.4}^{+0.5}$ [ATLAS] [29]	
	ggF	$0.73 \pm 0.50$ [CMS] [31]	
	VBF	$1.37_{-0.58}^{+0.56}$ [CMS] [31]	
	Vh	$0.75_{-1.40}^{+1.44}$ [CMS] [31]	
	Inclusive	$0.78 \pm 0.27$ [CMS] [32]	
	ggF	$2.1_{-1.9}^{+2.2}$ [Tevatron] [21]	

$$\chi^2 = \sum_{i=1}^{33} \left( \frac{R_i^{\text{LW}} - R_i^{\text{meas}}}{\sigma_i^{\text{meas}}} \right)^2, \quad (3.2)$$

where  $i$  runs over the 33 channels in Table 1.  $R_i^{\text{LW}}$  stands for the predicted strength in the model presented here,  $R_i^{\text{meas}}$  is the measured strength and  $\sigma_i^{\text{meas}}$  is the corresponding error. Asymmetric errors were averaged in quadrature,  $\sigma = \sqrt{(\sigma_+^2 + \sigma_-^2)}/2$ . Note that only experimental errors were taken into account; in most cases, theoretical errors cancel in the ratio of a given observable with its standard model expectation. In the cases where the cancellation is not exact, the theoretical uncertainty remains small. For example, an  $\mathcal{O}(10\%)$  theoretical uncertainty in the ggF production cross section does not entirely scale out the ratio of inclusive production cross sections; however, this translates into an  $\mathcal{O}(1\%)$  theoretical uncertainty in the ratio, which is much smaller than the current experimental error bars.

We determine the 95% C.L. lower bound on the heavy neutral Lee–Wick scalar mass using Eq. (3.2) and the  $\chi^2$  probability

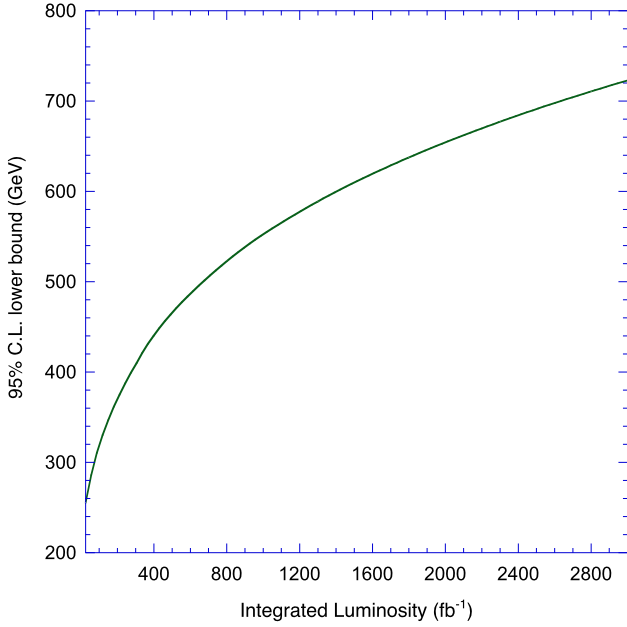


**Fig. 1.** Projected lower bound on the heavy Lee–Wick scalar mass  $m_{\tilde{h}_0}$  as a function of the LHC integrated luminosity.

distribution corresponding to 32 degrees of freedom. For the data in Table 1, which includes  $\sim 25 \text{ fb}^{-1}$  of LHC data at  $\sim 8 \text{ TeV}$ , we find

$$m_{\tilde{h}_0} > 255 \text{ GeV } 95\% \text{C.L.} \quad (3.3)$$

This corresponds to a mixing parameter  $\alpha \approx -0.25$ .

To estimate the future reach of the LHC, we follow the same procedure as in Ref. [15]. We assume that the experimental signal strengths will converge to their standard model values, namely  $R_i^{\text{meas}} = 1$ , and that the experimental error bars will shrink relative to their current values by a factor of  $1/\sqrt{N}$  where

$$N = \frac{\sigma_{14} L_{14}}{\sigma_8 L_8}. \quad (3.4)$$

Here,  $\sigma_X$  is the total Higgs production cross section at center-of-mass energy  $X$ , and  $L_X$  is the corresponding integrated luminosity. This scaling of errors as the inverse square root of the number of events was also done in Ref. [15], and corresponds to “scheme 2” of the CMS [17] high luminosity projections<sup>1</sup>.

The results of our projection are shown in Fig. 1. As one might expect, the lower bound on  $m_{\tilde{h}_0}$  increases monotonically with integrated luminosity; the left-most point on the curve corresponds to the current bound in Eq. (3.3), while the rest follow from our procedure for determining projected bounds at a 14 TeV LHC. For two benchmark points, we find

$$m_{\tilde{h}_0} > 420 \text{ GeV } 95\% \text{C.L.} \quad (L_{14} = 300 \text{ fb}^{-1}), \quad (3.5)$$

$$m_{\tilde{h}_0} > 720 \text{ GeV } 95\% \text{C.L.} \quad (L_{14} = 3000 \text{ fb}^{-1}) \quad (3.6)$$

corresponding to the mixing angles  $\alpha \approx -0.09$  and  $-0.03$ , respectively. We discuss the implications of these bounds in the final section.

<sup>1</sup> The assumption that the uncertainty scales as one over the square root of the number of events is true for the statistical error. Here we assume that a comparable reduction in the systematic errors is possible with increasing luminosity. This assumption may be optimistic, but is the one used by CMS for the European Strategy Report [17].

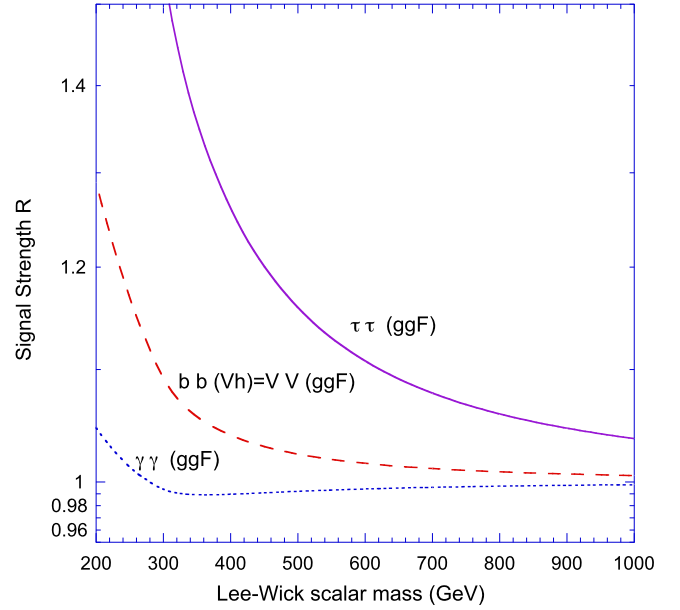


**Fig. 2.** Model predictions for the signal strengths  $R_i^{\text{LW}}$  as a function of  $m_{\tilde{h}_0}$ .

As the experimental uncertainties on the Higgs boson signal strengths become smaller, new physics in this model should become manifest by an emerging pattern of deviations from the standard model expectations. To illustrate this, we show in Fig. 2 some of the signal strengths expected in the Lee–Wick theory as a function of the heavy Lee–Wick scalar mass. The  $\tau\tau$  mode via ggF shows the greatest deviation from the standard model since both the production and decay width are each modified by the factor  $\exp(-2\alpha)$  which is larger than one. The signal strength for  $H \rightarrow VV$  decays is also enhanced. Although the deviation is not as great as the  $\tau\tau$  channel shown, there are very few extensions of the standard model that would lead to such an enhancement. Hence, this effect is a distinctive feature of the model that might be identified if the underlying physics is realized in nature.

#### 4. Conclusions

Now that the LHC has discovered a light, standard model-like Higgs boson and begun a study of its properties, one can examine the current and future constraints that can be placed on standard model extensions. In this Letter, we have considered such constraints on a Lee–Wick extension of the Higgs sector. Although most of the partners in the LWSM must be heavy, due to various low-energy constraints, the partners of the Higgs boson need not be. The resulting effective theory is a constrained two-Higgs doublet model, one in which some propagators and vertices have unusual signs. In addition, the mixing between the light Higgs and the heavy neutral scalar is described by a symplectic rotation, leading to hyperbolic functions of a mixing angle at the vertices. The mixing angle itself is related to the two neutral Higgs masses, and thus the heavy neutral scalar mass can be taken as the only free parameter. The charged and pseudoscalar Higgs masses are degenerate at tree level and are also determined once the heavy scalar mass has been specified.

We first considered the bounds from current LHC data, looking at 33 different signals, and found a 95% confidence level lower bound of 255 GeV on the heavy scalar mass. Extrapolating to the next runs at the LHC (at 14 TeV), we found that the bound will increase to 420 GeV (720 GeV) for an integrated luminosity of 300 (3000) inverse femtobarns. The first signature of a deviation will

come from light Higgs boson decays to either tau or massive gauge boson pairs. Unlike most extensions of the standard model, both of these signal strengths are greater than in the standard model.

In Ref. [8], it was shown that flavor constraints on the Lee–Wick charged Higgs provide a lower bound on the heavy neutral scalar mass. The 95% C.L. bounds on the charged Higgs from  $B_d - \bar{B}_d$ ,  $B_s - \bar{B}_s$  mixing and  $b \rightarrow X_s \gamma$  were found to be 303 GeV, 354 GeV and 463 GeV, respectively [8]. The most stringent of these bounds translates into a lower bound on the heavy neutral scalar of 445 GeV. We thus see that the current bound from  $b \rightarrow X_s \gamma$  is more stringent than those from current Higgs data, and that it will require approximately 400 femtobarns at a 14 TeV LHC in order to supersede this bound.

## Acknowledgements

The work of C.C. and R.R. was supported by the NSF under Grant PHY-1068008. The opinions and conclusions expressed herein are those of the authors, and do not represent the National Science Foundation.

## References

- [1] B. Grinstein, D. O’Connell, M.B. Wise, Phys. Rev. D 77 (2008) 025012.
- [2] T.D. Lee, G.C. Wick, Nucl. Phys. B 9 (1969) 209; T.D. Lee, G.C. Wick, Phys. Rev. D 2 (1970) 1033.
- [3] R.E. Cutkosky, P.V. Landshoff, D.I. Olive, J.C. Polkinghorne, Nucl. Phys. B 12 (1969) 281.
- [4] S. Coleman, in: Subnuclear Phenomena, Ettore Majorana School, Erice, 1969, Academic Press, New York, 1970, pp. 282–327.
- [5] B. Grinstein, D. O’Connell, M.B. Wise, Phys. Rev. D 79 (2009) 105019.
- [6] E. Alvarez, L. Da Rold, C. Schat, A. Szykman, J. High Energy Phys. 0910 (2009) 023; C.D. Carone, Phys. Lett. B 730 (2014) 1, arXiv:1312.0702 [hep-ph].
- [7] F.A. Barone, G. Flores-Hidalgo, A.A. Nogueira, arXiv:1311.2040 [hep-th]; R.F. Lebed, A.J. Long, R.H. TerBeek, Phys. Rev. D 88 (2013) 085014; K. Bhattacharya, Y.-F. Cai, S. Das, Phys. Rev. D 87 (2013) 083511; M. Dias, A.Y. Petrov, C.R. Senise Jr., A.J. da Silva, arXiv:1212.5220; I. Cho, O.-K. Kwon, Eur. Phys. J. C 73 (2013) 2341; I. Cho, O.-K. Kwon, Phys. Rev. D 82 (2010) 025013; R.F. Lebed, R.H. TerBeek, Phys. Rev. D 87 (2013) 015006; R.F. Lebed, R.H. TerBeek, J. High Energy Phys. 1209 (2012) 099; N. Kan, K. Kobayashi, K. Shiraiishi, Acta Phys. Pol. B 44 (2013) 721; K. Bhattacharya, S. Das, Phys. Rev. D 86 (2012) 025009; K. Bhattacharya, S. Das, Phys. Rev. D 84 (2011) 045023; R.S. Chivukula, A. Farzinnia, R. Foadi, E.H. Simmons, Phys. Rev. D 82 (2010) 035015; C.D. Carone, Phys. Lett. B 677 (2009) 306; A. Rodigast, T. Schuster, Phys. Rev. D 79 (2009) 125017; B. Fornal, B. Grinstein, M.B. Wise, Phys. Lett. B 674 (2009) 330; C.D. Carone, R.F. Lebed, J. High Energy Phys. 0901 (2009) 043; T.G. Rizzo, J. High Energy Phys. 0706 (2007) 070; T.G. Rizzo, J. High Energy Phys. 0801 (2008) 042; E. Gabrielli, M. Raidal, arXiv:1310.1090 [hep-ph].
- [8] C.D. Carone, R. Primulando, Phys. Rev. D 80 (2009) 055020.
- [9] E. Alvarez, E.C. Leskow, J. Zurita, Phys. Rev. D 83 (2011) 115024, arXiv:1104.3496 [hep-ph].
- [10] T. Figy, R. Zwicky, J. High Energy Phys. 1110 (2011) 145.
- [11] R.S. Chivukula, A. Farzinnia, R. Foadi, E.H. Simmons, Phys. Rev. D 81 (2010) 095015, arXiv:1002.0343 [hep-ph]; T.E.J. Underwood, R. Zwicky, Phys. Rev. D 79 (2009) 035016, arXiv:0805.3296 [hep-ph]; E. Alvarez, L. Da Rold, C. Schat, A. Szykman, J. High Energy Phys. 0804 (2008) 026, arXiv:0802.1061 [hep-ph]; C.D. Carone, R.F. Lebed, Phys. Lett. B 668 (2008) 221, arXiv:0806.4555 [hep-ph].
- [12] LHC Higgs Cross Section Working Group, in: S. Heinemeyer, C. Mariotti, G. Passarino, R. Tanaka (Eds.), Handbook of LHC Higgs Cross Sections: 3. Higgs Properties, CERN, Geneva, 2013, CERN-2013-004, arXiv:1307.1347 [hep-ph].
- [13] J.F. Gunion, H.E. Haber, G.L. Kane, S. Dawson, Front. Phys. 80 (2000) 1.
- [14] C.-Y. Chen, S. Dawson, Phys. Rev. D 87 (5) (2013) 055016, arXiv:1301.0309 [hep-ph].
- [15] C.-Y. Chen, S. Dawson, M. Sher, Phys. Rev. D 88 (2013) 015018, arXiv:1305.1624 [hep-ph].
- [16] P.M. Ferreira, R. Santos, M. Sher, J.P. Silva, Phys. Rev. D 85 (2012) 077703, arXiv:1112.3277 [hep-ph]; D.S.M. Alves, P.J. Fox, N.J. Weiner, arXiv:1207.5499 [hep-ph]; N. Craig, S. Thomas, J. High Energy Phys. 1211 (2012) 083, arXiv:1207.4835 [hep-ph]; N. Craig, J.A. Evans, R. Gray, C. Kilic, M. Park, S. Somalwar, S. Thomas, J. High Energy Phys. 1302 (2013) 033, arXiv:1210.0559 [hep-ph]; Y. Bai, V. Barger, L.L. Everett, G. Shaughnessy, Phys. Rev. D 87 (2013) 115013, arXiv:1210.4922 [hep-ph]; A. Azatov, J. Galloway, Int. J. Mod. Phys. A 28 (2013) 1330004, arXiv:1212.1380; B.A. Dobrescu, J.D. Lykken, J. High Energy Phys. 1302 (2013) 073, arXiv:1210.3342 [hep-ph]; P.M. Ferreira, R. Santos, H.E. Haber, J.P. Silva, Phys. Rev. D 87 (5) (2013) 055009, arXiv:1211.3131 [hep-ph]; A. Celis, V. Ilisie, A. Pich, J. High Energy Phys. 1307 (2013) 053, arXiv:1302.4022 [hep-ph]; B. Grinstein, P. Uttayarat, J. High Energy Phys. 1306 (2013) 094, arXiv:1304.0028 [hep-ph]; B. Grinstein, P. Uttayarat, J. High Energy Phys. 1309 (2013) 110 (Erratum); M. Krawczyk, D. Sokolowska, B. Swiezewska, J. Phys. Conf. Ser. 447 (2013) 012050, arXiv:1303.7102 [hep-ph]; B. Coleppa, F. Kling, S. Su, arXiv:1305.0002 [hep-ph]; W. Altmannshofer, S. Gori, G.D. Kribs, Phys. Rev. D 86 (2012) 115009, arXiv:1210.2465 [hep-ph]; C.-W. Chiang, K. Yagyu, J. High Energy Phys. 1307 (2013) 160, arXiv:1303.0168 [hep-ph]; L. Basso, A. Lipniacka, F. Mahmoudi, S. Moretti, P. Osland, G.M. Pruna, M. Pirmohammadi, J. High Energy Phys. 1211 (2012) 011, arXiv:1205.6569 [hep-ph]; J. Chang, K. Cheung, P.-Y. Tseng, T.-C. Yuan, Phys. Rev. D 87 (3) (2013) 035008, arXiv:1211.3849 [hep-ph]; N. Craig, J. Galloway, S. Thomas, arXiv:1305.2424 [hep-ph]; L. Wang, X.-F. Han, arXiv:1312.4759 [hep-ph]; CMS Collaboration, CMS-PAS-FTR-13-024; S. Chang, S.K. Kang, J.-P. Lee, K.Y. Lee, S.C. Park, J. Song, arXiv:1310.3374 [hep-ph]; O. Eberhardt, U. Nierste, M. Wiebusch, J. High Energy Phys. 1307 (2013) 118, arXiv:1305.1649 [hep-ph].
- [17] CMS Collaboration, CMS Note 2012-006.
- [18] ATLAS Collaboration, ATLAS-CONF-2013-012.
- [19] G. Aad, et al., ATLAS Collaboration, Phys. Lett. B 726 (2013) 88, arXiv:1307.1427 [hep-ex].
- [20] CMS Collaboration, CMS PAS HIG-13-001.
- [21] See talk slides, ‘H  $\rightarrow$  bb from Tevatron’, by Yuji Enari, at HCP2012.
- [22] ATLAS Collaboration, ATLAS-CONF-2013-030.
- [23] CMS Collaboration, CMS PAS HIG-13-003.
- [24] S. Chatrchyan, et al., CMS Collaboration, J. High Energy Phys. 1401 (2014) 096, arXiv:1312.1129 [hep-ex].
- [25] CMS Collaboration, CMS PAS HIG-13-002.
- [26] S. Chatrchyan, et al., CMS Collaboration, arXiv:1312.5353 [hep-ex].
- [27] ATLAS Collaboration, ATLAS-CONF-2013-079.
- [28] S. Chatrchyan, et al., CMS Collaboration, Phys. Rev. D 89 (2014) 012003, arXiv:1310.3687 [hep-ex].
- [29] ATLAS Collaboration, ATLAS-CONF-2013-108.
- [30] ATLAS Collaboration, ATLAS-CONF-2012-160.
- [31] CMS Collaboration, CMS PAS HIG-13-004.
- [32] S. Chatrchyan, et al., CMS Collaboration, arXiv:1401.5041 [hep-ex].